



Published in final edited form as:

J Am Chem Soc. 2019 August 14; 141(32): 12824–12831. doi:10.1021/jacs.9b05912.

BODIPY Fluorophores for Membrane Potential Imaging

Jenna M. Franke[‡], Benjamin K. Raliski[‡], Steven C. Boggess[‡], Divya V. Natesan[‡], Evan T. Koretsky[‡], Patrick Zhang[‡], Rishikesh U. Kulkarni[‡], Parker E. Deal[‡], Evan W. Miller^{‡,§,†,*}

[‡]Department of Chemistry, University of California, Berkeley, California 94720, United States.

[§]Department of Molecular & Cell Biology, University of California, Berkeley, California 94720, United States.

[†]Department of Helen Wills Neuroscience Institute. University of California, Berkeley, California 94720, United States.

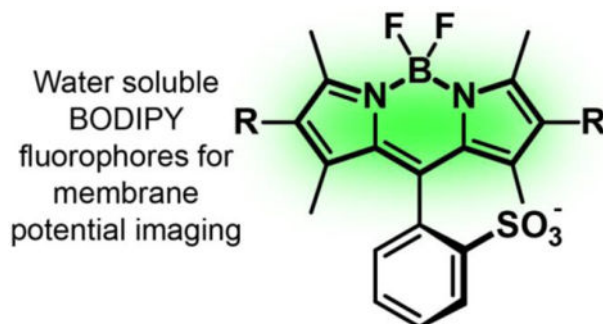
Abstract

Fluorophores based on the BODIPY scaffold are prized for their tunable excitation and emission profiles, mild syntheses, and biological compatibility. Improving the water-solubility of BODIPY dyes remains an outstanding challenge. The development of water-soluble BODIPY dyes usually involves direct modification of the BODIPY fluorophore core with ionizable groups or substitution at the boron center. While these strategies are effective for the generation of water-soluble fluorophores, they are challenging to implement when developing BODIPY-based indicators: direct modification of BODIPY core can disrupt the electronics of the dye, complicating the design of functional indicators; and substitution at the boron center often renders the resultant BODIPY incompatible with the chemical transformations required to generate fluorescent sensors. In this study, we show that BODIPYs bearing a sulfonated aromatic group at the *meso* position provide a general solution for water-soluble BODIPYs. We outline the route to a suite of 5 new sulfonated BODIPYs with 2,6-disubstitution patterns spanning a range of electron-donating and -withdrawing propensities. To highlight the utility of these new, sulfonated BODIPYs, we further functionalize them to access 13 new, BODIPY-based voltage-sensitive fluorophores. The most sensitive of these BODIPY VF dyes displays a 48% $\Delta F/F$ per 100 mV in mammalian cells. Two additional BODIPY VFs show good voltage sensitivity (24% $\Delta F/F$) and excellent brightness in cells. These compounds can report on action potential dynamics in both mammalian neurons and human stem cell-derived cardiomyocytes. Accessing a range of substituents in the context of a water soluble BODIPY fluorophore provides opportunities to tune the electronic properties of water-soluble BODIPY dyes for functional indicators.

Graphical Abstract

*Corresponding Author: evanwmiller@berkeley.edu.

Supporting Information. Support figures, spectra, synthetic methods and imaging details. This material is available free of charge via the Internet at <http://pubs.acs.org>.



Introduction

Synthetic chemistry has long been a source of colorful compounds¹⁻³ whose ability to absorb light enable applications in far-ranging fields. Fluorescent dyes find wide-spread use in the modern research laboratory where features such as visible excitation and emission profiles, large molecular brightness values, and photostability are highly prized, along with biologically-compatible properties like water-solubility. Since the late 19th century, xanthenes dyes like fluoresceins⁴ and rhodamines⁵⁻⁶ offered a fertile source of inspiration as scaffolds for biologically-useful dyes and indicators.⁷⁻⁹ More recently, BODIPY, or 4,4-difluoro-4-bora-3a,4a,-diazas-indacene, (Scheme 1) dyes have emerged as a versatile complement to xanthenes dyes. Owing to the relatively mild reaction conditions for the generation of BODIPY fluorophores,¹⁰ a number of flexible synthetic routes afford the opportunity to install a range of substituents directly to the BODIPY core, tuning both the color and electronic properties of BODIPY dyes.

Since the initial report of BODIPY in 1968,¹¹ a proliferation of synthetic methods^{10, 12-13} and conceptual understanding¹⁴⁻¹⁵ enabled the application of BODIPYs as indicators for a number of important, biologically-relevant analytes and properties,¹⁶⁻¹⁷ including pH,¹⁸⁻¹⁹ cations like Na⁺,²⁰⁻²¹ K⁺,^{20, 22} Mg²⁺,²³ and Ca²⁺,²⁴⁻²⁵ transition metals;²⁶⁻²⁸ reactive oxygen²⁹ and nitrogen species,¹⁴ electron transfer reactions,³⁰ and membrane viscosity.³¹ Because of the broad tunability of BODIPY-based scaffolds, we thought these fluorophores would make an excellent choice for incorporation into a molecular wire-based, photo-induced electron transfer (PeT) membrane potential sensing framework.³² Previous work in our lab showed that tuning the relative electron affinities between a fluorescein-based reporter and electronically-orthogonal phenylenevinylene molecular wire voltage-sensing domain profoundly altered the voltage sensitivities of fluorescein based dyes. However, the limited synthetic scope of sulfonated fluorescein only allowed access to a narrow range of substituents (H, F, Cl, Me).³³

Here, we introduce new, water-soluble sulfonated BODIPYs with substituents ranging from highly electron donating (R = Et) to withdrawing (R = CN). We incorporate the new, sulfonated BODIPYs into a molecular wire voltage-sensing scaffold to provide the first examples of PeT-based voltage-sensitive BODIPYs. The most sensitive of these dyes displays a 48% F/F per 100 mV in HEK cells, and two others possess 24% F/F, making them useful for voltage sensing applications in both neurons and cardiomyocytes.

Design of water soluble BODIPYs

We prepared a total of 13 BODIPY-based Voltage-sensitive Fluorophores, or BODIPY-VF dyes. All of the BODIPY compounds feature a common *ortho*-sulfonic acid substituted *meso* aromatic ring (8-position, Scheme 1) and substitution patterns at the 2,6 positions that include hydrogen, ethyl, carboxylate, amide, and cyano functionalities (Scheme 1). Our initial attempts to access BODIPY-based VoltageFluor indicators centered around the development of water-soluble tetramethyl, diethyl BODIPY fluorophores. Ionizable groups, such as sulfonates or carboxylates, are essential for the proper orientation of VF-type dyes in cellular membranes.^{34–35} We first sought to introduce water-solubilizing groups centered on substitution at boron.^{36–38} However, in our hands, these modifications proved incompatible with the Pd-catalyzed Heck coupling for installation of voltage-sensing phenylenevinylene molecular wires. Functionalization of the 2 and 6 positions of the BODIPY core offered a route to the installation of water-solubilizing groups like sulfonates^{39–40} or carboxylates,⁴¹ but direct functionalization of the BODIPY core can profoundly alter redox properties, confounding the tuning of fluorophore redox potential^{15, 33} with installation of water solubilizing groups. One solution is to include a sulfonate on the *meso* aromatic ring (Scheme 1), which we hypothesized would improve solubility, be generalizable across a range of 2,6-substitution patterns on the BODIPY core, and aid in the proper orientation within cellular plasma membranes.

Synthesis of H- and Et-BODIPY VoltageFluors

Owing to the commercial availability of the 3-ethyl-2,4-dimethyl-*IH*-pyrrole precursors (kryptopyrrole), we first synthesized BODIPY **3** and **11** (Scheme 2) for use in subsequent coupling with phenylenevinylene molecular wires. The sulfonated benzaldehyde precursor, **9** (Scheme 2, and related *para*-isomer, **1**, Scheme 2), was completely insoluble in CH₂Cl₂ and toluene, the most commonly used solvents for BODIPY condensations.^{10, 14, 20, 31, 42–45} We screened polar solvents for the TFA-catalyzed condensation of aldehyde **9** (or **1**) with kryptopyrrole **2** (Scheme 2). DMF gave the best conversion to the dipyrromethane. Oxidation with DDQ to form the corresponding dipyrromethene followed by BF₃ chelation with boron trifluoride diethyl etherate (BF₃·OEt₂) in CH₂Cl₂ solvent gave *ortho*-sulfonated BODIPY **3** (Br *para* to BODIPY, Scheme 2) in 49% yield and **11** (Br *meta* to BODIPY, Scheme 2) in 33% yield.

A Pd-catalyzed Heck coupling between BODIPY **3** and substituted styrenes **4** and **5** gave two different 2,6-diethyl, *para* molecular wire BODIPY VoltageFluors: Et*p*H (**6**) and Et*p*OMe (**7**) in 92 and 25% isolated yield, respectively (Scheme 2). The naming convention represents the ethyl groups at the 2,6-positions, molecular wire *para* from the fluorophore, and the identity of the R₁ substituent. Derivatives with the molecular wire *meta* from the fluorophore were prepared via a similar route from BODIPY **11** (Scheme 2; Et*m*H **15**, 26% yield, and Et*m*OMe **16**, 29%). Tetramethyl BODIPY VoltageFluors **17–19** (R = H) were prepared first by reacting 2,4-dimethyl-*IH*-pyrrole **10** with sulfonated aldehyde **9**, resulting in a 38% yield of *ortho*-sulfonated tetramethyl BODIPY **12**. Heck coupling with substituted styrene **4**, **13**, or **14** then gave TM*m*H (**17**), TM*m*Me (**18**), and TM*m*OMe (**19**) in 35% yield after silica gel chromatography.

Synthesis of CN-BODIPY VoltageFluor

Access to electron-withdrawing BODIPY derivatives provide a useful counterpoint to H- and ethyl-substituted BODIPYs and may produce lower levels of reactive $^1\text{O}_2$ than more electron-rich derivatives.⁴¹ Synthesis of cyano VoltageFluor derivative **22** was more challenging than either H- or Et-substituted BODIPY VoltageFluors. Because of the poor nucleophilicity of 2,4-dimethyl-*1H*-pyrrole-3-carbonitrile (**20**), no reaction with sulfonated benzaldehyde **9** was observed unless heated to 60 °C. The heated condensation resulted in only an 8% isolated yield of **21**. Switching the solvent to a 2:3 DMF:CH₂Cl₂ mixture and adding an excess of TFA (100 μL, 6 equiv.) allowed the synthesis to proceed at room temperature and increased the isolated yield to 29% (Scheme 2).

BODIPY **21** is less stable than BODIPYs **11** and **12**, possibly due to the lower effective charges on the dipyrromethene nitrogen atoms.⁴⁶ When subjected to the Pd-catalyzed Heck coupling conditions that afforded previous BODIPY VF dyes, BODIPY **21** decomposed before conversion to product. Lowering the reaction temperature from 100 °C to 70 °C did not prevent decomposition. By exposing BODIPY **21** to Heck reaction conditions and systematically removing single reaction components, we determined that the presence of trimethylamine (NEt₃) was initiating decomposition of BODIPY **21**. Replacing NEt₃ with inorganic bases (Cs₂CO₃, K₂CO₃) or bulky amine bases (1,8-bis(dimethylamino)naphthalene) resulted in scant improvement in conversion; decomposition of **21** remained a problem. To circumvent the sensitivity of BODIPY **21**, we attempted a base-free Heck coupling, relying only on the substituted aniline of styrene reactant **4** to buffer generated HBr. The resulting Heck coupling was low yielding (6%), but provided sufficient **22** to purify and characterize (Scheme 2).

Synthesis of dicarboxy- and diamido-BODIPY VoltageFluors

The 2,6-dicarboxy VoltageFluor series was synthesized via two different routes. Initially, BODIPY **32** was synthesized in a 49% yield from aldehyde **9** and 2,4-dimethylpyrrole-3-carboxylic acid **31** (Scheme 3), then subjected to the same base-free Heck coupling conditions as the BODIPY **21**, giving the 2,6-dicarboxylic acid VoltageFluor, **28** in a 6% yield after preparative thin layer chromatography (pTLC). Subsequent Heck couplings with unprotected BODIPY **32** gave inconsistent results: either unmodified starting material or decomposition. We suspected the carboxylates could be chelating the palladium catalyst and decided to switch to a protecting group approach, which would likely improve the Heck coupling and allow for more facile purification of intermediates by normal phase chromatography.

Benzyl ester protected pyrrole **23** is less nucleophilic than its carboxylic acid precursor. We performed the BODIPY condensation in 2:3 DMF:CH₂Cl₂, providing benzyl-protected BODIPY **24** in a 61% isolated yield (Scheme 3). Benzyl-protected BODIPY **24** proceeds cleanly through Heck coupling, even in the presence of NEt₃. Benzyl-protected intermediates **26** and **27** were isolated in a 30 and 43% yield following column chromatography. Cleavage of the benzyl groups with Pd/C under hydrogen atmosphere also reduced one of the alkenes of the molecular wire, evidenced by a mass 2 m/z higher than the

desired product (Figure S1) and increased brightness of the resulting dye. A Birkofer reduction^{47–48} with Pd(OAc)₂, Et₃SiH, NEt₃ in CH₂Cl₂ at room temperature gave the cleanest conversion to the free carboxylate product with minimal over-reduction of the alkenes of the molecular wire. BODIPY VF dyes **29** and **30** were isolated in 31 and 14% yield after pTLC.

BODIPY VoltageFluors **35** and **36** were synthesized via Heck coupling between styrenes **4** or **13** and BODIPY **34**, which was accessed in 82% yield from a HATU-mediated amide bond formation between BODIPY **32** and glycine methyl ester **33**. Like benzyl-protected BODIPY **24**, the amide-substituted BODIPY withstands the presence of NEt₃ in the Pd-catalyzed cross-coupling, which returns **35** and **36** in 21% and 34% isolated yields, respectively (Scheme 3).

Spectroscopic characterization of sulfonated BODIPYs

The absorption and the emission of BODIPY fluorophores (Figure 1, Table 1) and VoltageFluors (Figure 2a, Figure S2, Table 2) varied with the 2,6-substituents. Consistent with a Dewar formalism,^{49–51} electron-withdrawing groups at the 2,6-positions result in a hypsochromatic shift ($\lambda_{\text{max}} = 502$ nm for BODIPY **21**) and electron donating groups like Et (BODIPY **3** and **11**) yield bathochromic shifts ($\lambda_{\text{max}} = 530$ nm). Emission trends mirror the absorption profiles, with the electron-rich BODIPYs **3** and **11** emitting around 544 nm, and BODIPY **21**, the most electron-poor, emitting at 517 nm. The absorption and emission profiles of the complete BODIPY VF dyes (acquired in ethanol to improve solubility of the complete BODIPY VF dyes) closely match the spectra of the parent BODIPY fluorophores, with absorption profiles centered at 502 to 528 nm and the phenylene vinylene molecular wire absorbing near 400 nm (Figure 2a, Figure S2, and Table 2). The *ortho*-sulfonated BODIPY fluorophores have impressive fluorescence quantum yields (ϕ_{fl}) of 0.70–0.99 (Table 1), but after the addition of the phenylene vinylene molecular wire the quantum yields drop dramatically, supporting the presence of PeT within the compounds (Table 2). The absorption spectra of BODIPY VF dyes **17**, **18**, and **19** closely match the excitation spectra (Figure S3a–c). The BODIPY region of the absorbance spectra of **17–19** does not change from pH 2.5 to 10 (Figure S3d–f). However, the emission of **17–19** increases up to 20-fold at pH 2.5, consistent with a PeT-based mechanism of fluorescence enhancement (Figure S3g–i).

Cellular performance of BODIPY VF Dyes

All BODIPY VF dyes localize to cell membranes (Figure 2b, Figure S4a,b–S9a,b) and display different cellular brightness (Table 2, Figure S10a). Despite having the highest ϕ_{fl} , **6** was one of the dimmest dyes in cells (relative brightness in cells = 0.4, compared to **19**), likely due to its poor solubility in aqueous buffer even in the presence of detergent (Table 2). On the other hand, BODIPY VF dyes **28–30** possessed the largest cellular brightness (relative brightness up to 12x, Table 2, Figure S10a). We speculate that the increased anionic character of BODIPY VFs **28–30**, with three negative charges, improves the water solubility of the dyes, enabling more efficient delivery to cellular membranes.

After confirming BODIPY VF dyes localize to the cell membrane, we next investigated their voltage sensitivity using whole cell voltage-clamp electrophysiology in tandem with epifluorescence microscopy (Figure 2c,d Figure S4c,d–S9c,d). We stepped the membrane potential of a single HEK cell stained with 2 μ M BODIPY VF from a holding potential of -60 mV to ± 100 mV while recording dye fluorescence intensity. BODIPY VF dyes **6**, **7**, **15**, and **16** demonstrate little to no voltage sensitivity. BODIPY VF dyes **6** and **7**, with a *para* molecular wire configuration, show no voltage sensitivity (Figure S4c), while BODIPY VF dyes **15** and *Et*mOMe **16** display modest voltage sensitivities of 1.5 and 5 % F/F per 100 mV (Figure S5c,d and Table 2).

We hypothesized replacing the 2,6-diethyl BODIPY with progressively more electron-poor BODIPYs would increase PeT and therefore increase % F/F. Gratifyingly, we see a 67% increase in voltage sensitivity from **16** to **17**, from 1.5 to 2.5 % F/F (Figure S6c,d and Table 2). Strengthening the electron-donating ability of the aniline by addition of a methyl or methoxy group increased the voltage-sensitivity to 6.2 % for **18** and 33 % F/F for **19** (Figure 2).

More electron-deficient BODIPY VF **22** displayed extremely low cellular brightness (Table 2, Figure S7b, S10a) and required increasing both illumination intensity and camera exposure time in order to obtain a reasonable estimate of its voltage sensitivity, which was low: 3.8 % F/F per 100 mV (Table 2, Figure S7c,d). While BODIPY VF **22** was slightly more voltage sensitive than its analogous precursors, **15** and **17**, its extremely low cellular brightness prohibited further use as a voltage-sensitive dye in cells.

We then evaluated the 2,6-dicarboxy and diamido BODIPY series, hoping to find an electronic “sweet spot” between the tetramethyl and cyano series. The BODIPY VF dyes **28**, **29**, and **30** had voltage sensitivities of 4.4%, 9.9%, and 24% F/F per 100 mV, respectively (Figure S8c,d and Table 2). While dicarboxy BODIPY VF dyes display a similar range of voltage sensitivities to their tetramethyl precursors, the most striking quality of the dicarboxy BODIPY VF dyes was their cellular brightness—they were 5–12x brighter compared to the cellular fluorescence intensity of **19** (Table 2, all cellular brightness values normalized to **19**). The *in vitro* fluorescence quantum yields of the carboxy BODIPY VF dyes are slightly lower than the tetramethyl BODIPY VF dyes, so this increase in brightness is likely due to improved hydrophilicity and cell loading efficiency. We found that amide-substituted BODIPY VF **35** (Figure S9c,d) possesses voltage sensitivity 10x greater than the corresponding **28**, with a fractional sensitivity of 48% F/F per 100 mV in HEK cells (compared to 4.4% for **28**). Introduction of a more electron-rich molecular wire (methyl substitution) results in a loss of voltage sensitivity for **36**, which displays only nominal voltage sensitivity (5.1% F/F per 100 mV).

Functional Imaging in Neurons and Cardiomyocytes

We evaluated the ability of BODIPY VF dyes to report on voltage dynamics in electrically excitable cells: mammalian neurons and human induced pluripotent stem cell-derived cardiomyocytes (hiPSC-CMs). Three BODIPY VoltageFluors stood out as good candidates for functional imaging: **19** and **35** because of their high F/F (33 and 48%, respectively),

and **30** because of its combination of cellular brightness (7x brighter than **19** and **35**) and good sensitivity (24% F/F).

We evaluated the photostability of these BODIPY VF dyes in HEK cells. Based on previous reports,⁴¹ we predicted photostability would decrease from **35** > **19** > **30**. Indeed, we find BODIPY VF **35** to be the most photostable in HEK cells, maintaining near 100% fluorescence after 6 min of constant illumination, although with some photobrightening (Figure S10b). BODIPY VF **19** displays photostability comparable to fluorescein-based VF2.1.Cl³² (Figure S10b). Carboxy-substituted BODIPY **30** bleaches the most rapidly, dropping to about 20% of original fluorescence values after 2 minutes (Figure S10b). However, because of the high starting brightness of BODIPY VF **30**, this indicator retains its utility for functional voltage imaging.

In cultured rat hippocampal neurons stained with BODIPY VFs, both **19** and **35** were too dim to capture evoked neuronal action potentials with sufficient signal-to-noise. BODIPY VF **30** displayed bright, membrane-localized staining in neurons isolated from rat hippocampi (Figure 3a and b). BODIPY VF **30** responded to electrically-evoked neuronal action potentials (Figure 3c and d), which could be detected when analyzing single cell regions of interest (ROIs) or when viewing the entire field of neurons.

We also evaluated the performance of BODIPY VF dyes **19**, **30**, and **35** in human induced pluripotent stem cell-derived cardiomyocytes (hiPSC-CMs). All three BODIPY VFs stain the membranes of hiPSC-CMs (Figure 4a, Figure S11). High-speed fluorescence microscopy (200 Hz frame rate) demonstrates that all three BODIPY VFs can report on spontaneously-generated cardiac action potentials in hiPSC-CMs (Figure 4 and Figure S11) during 10 second bouts of imaging.

We found BODIPY VF **19** was the best suited voltage reporter because of its robust 33% F/F and good signal-to noise (Figure 4c). Additionally, under longer-term imaging (60 sec of continuous imaging), **19** displays the least phototoxic effects among the BODIPYs tested under constant illumination. Under these conditions, the photostability of BODIPY VF **19** was comparable to VF2.1.Cl,³² although with lower signal to noise than either VF2.1.Cl or fVF 2⁵² (Figure S12). Like VF2.1.Cl, BODIPY VF **19** also slightly alters the shape and magnitude of cardiac action potentials under prolonged illumination (Figure S12). These effects are not seen during shorter imaging sessions (Figure 4d).

Discussion

We designed and synthesized 5 new sulfonated BODIPY dyes with variable 2,6-substitution patterns. These sulfonated fluorophores represent a generalizable solution to improving BODIPY water solubility while simultaneously avoiding modification to the boron center or fluorophore core. We incorporated these fluorophores into 13 new BODIPY voltage-sensitive fluorophores for evaluation in live-cell imaging, but the tunable, water-soluble BODIPYs presented here may have applications beyond voltage sensing. BODIPY VF **35** is the most sensitive BODIPY-based voltage indicator to date,⁵³⁻⁵⁴ but its low cellular brightness precludes its ready adoption for functional imaging in electrically excitable cells

like neurons or cardiomyocytes. Two other indicators developed in this study, BODIPY VF **19**, with its slightly lower sensitivity (33% F/F per 100 mV), but good brightness, and BODIPY VF **30**, which retains good voltage sensitivity (24% F/F per 100 mV) and exceptional brightness (~7x brighter than **19** or **35**) are better suited for functional imaging in cardiomyocytes or neurons, where they can each report on action potential dynamics in single trials.

The voltage sensitivity of the BODIPY VF dyes correlates with the electron-withdrawing character of the 2,6-substitution pattern in the BODIPY fluorophore. More electron-withdrawing substituents increase voltage sensitivity in the order of $-\text{Et} < -\text{H} < -\text{CO}_2\text{H} < -\text{CONHR} > -\text{CN}$. The extremely electron-withdrawing character of nitrile substitution makes for a poorly sensitive BODIPY VF. We find that calculated values of HOMO energies (Figure S13) for the BODIPY fluorophores—lacking the molecular wire—correlate extremely well with either *meta* or *para* Hammett constants (σ_m or σ_p),⁵⁵ validating the use of tabulated Hammett constants for analysis of the relative electron density of a particular BODIPY fluorophore (Figure S14a and b). Correlation between calculated HOMO energies and σ_m or σ_p values is best when evaluating neutral BODIPYs (Et, H, CONHR, or CN), with correlation coefficients (R^2) >0.99 for both σ_m and σ_p compared to HOMO. If carboxy-substituted BODIPYs are included, the correlation (R^2) between HOMO level and Hammett parameter drops to 0.92 (σ_m) and 0.78 (σ_p) (Figure S14a and b).

The average F/F for a class of BODIPY fluorophore (R = Et, H, CO₂H, CONHR, or CN) displays a parabolic relationship with calculated HOMO energy levels (Figure S14c), with maximum voltage sensitivity at around -4.75 eV (or $\sigma = 0.2 - 0.4$). BODIPY VF dyes that have very large and negative σ (GPeT,¹⁴ either by a combination of electron deficient fluorophores (R = CN) with mildly donating anilines (R = H) as in the case of BODIPY VF **22**, or by with moderately withdrawing fluorophores (R = CONHR) with electron-rich anilines (R = Me) in the case of BODIPY **35**, will have low voltage sensitivity. These results suggest that **35** occupies a “sweet spot” of PeT to optimize the voltage sensitivity for BODIPY VoltageFluors, and any further lowering of the fluorophore HOMO (such as amide BODIPY to cyano BODIPY) or raising the HOMO of the aniline PeT donor (unsubstituted aniline to methyl-substituted aniline) is detrimental to the voltage sensitivity.

Despite its impressive 48% F/F of BODIPY **35** in HEK cells, its low cellular brightness (12x less bright than dicarboxy BODIPY VFs) precludes its direct use in functional imaging. The low cellular brightness likely results from poor solubility of the dye, because the highly charged dicarboxy BODIPY VFs displayed greater cellular brightness. The structure of the diamido BODIPY VFs lend themselves to introduction of additional water-solubilizing groups, without significantly perturbing the electronics of the 2,6-diamide substitution pattern. Experiments are underway to expand the utility of amide-substituted BODIPYs in the context of voltage imaging and beyond.

Supplementary Material

Refer to Web version on PubMed Central for supplementary material.

ACKNOWLEDGMENT

Research in the Miller lab is supported by the National Institutes of Health (R35GM119855). J.M.F, B.K.R., S.C.B., and R.U.K. were supported in part by a training grant from the National Institutes of Health (T32GM066698). We thank Dr. Kathy Durkin and Dr. David Small for assisting with calculations performed in the Molecular Graphics and Computation Facility in the UC Berkeley College of Chemistry (NIH S10OD023532).

REFERENCES

1. Perkin WH, Producing a New Coloring Matter for Dyeing with a Lilac or Purple Color Stuffs of Silk, Cotton, Wool, or other Materials. British Patent 1856, No. 1984.
2. Cliffe WH, In the Footsteps of Perkin. *Journal of the Society of Dyers and Colourists* 1956, 72 (12), 563–566.
3. Welham RD, The Early History of the Synthetic Dye Industry*. *Journal of the Society of Dyers and Colourists* 1963, 79 (3), 98–105.
4. Baeyer A, Ueber eine neue Klasse von Farbstoffen. *Berichte der deutschen chemischen Gesellschaft* 1871, 4 (2), 555–558.
5. Ceresole M, Verfahren zur Darstellung von Farbstoffen aus der Gruppe des Meta-amidophenolphthaleins. German Patent 1887, No. 44002.
6. Sandmeyer T, Red dye. US Patent 1896, No. US573299A.
7. Tsien RY, Building and breeding molecules to spy on cells and tumors. *FEBS Lett* 2005, 579 (4), 927–32. [PubMed: 15680976]
8. Lavis LD; Raines RT, Bright building blocks for chemical biology. *ACS Chem Biol* 2014, 9 (4), 855–66. [PubMed: 24579725]
9. Lavis LD, Teaching Old Dyes New Tricks: Biological Probes Built from Fluoresceins and Rhodamines. *Annu Rev Biochem* 2017, 86 (1), 825–843. [PubMed: 28399656]
10. Loudet A; Burgess K, BODIPY dyes and their derivatives: syntheses and spectroscopic properties. *Chem Rev* 2007, 107 (11), 4891–932. [PubMed: 17924696]
11. Treibs A; Kreuzer FH, Di- and Tri-Pyrrylmethene Complexes with Di-Fluoro Boron. *Liebigs Ann Chem* 1968, 718 (12), 208–+.
12. Ziessel R; Ulrich G; Harriman A, The chemistry of Bodipy: a new El Dorado for fluorescence tools. *New J Chem* 2007, 31 (4), 496–501.
13. Ulrich G; Ziessel R; Harriman A, The chemistry of fluorescent bodipy dyes: Versatility unsurpassed. *Angew Chem Int Edit* 2008, 47 (7), 1184–1201.
14. Gabe Y; Urano Y; Kikuchi K; Kojima H; Nagano T, Highly Sensitive Fluorescence Probes for Nitric Oxide Based on Boron Dipyrromethene Chromophore-Rational Design of Potentially Useful Bioimaging Fluorescence Probe. *J Am Chem Soc* 2004, 126 (10), 3357–3367. [PubMed: 15012166]
15. Lincoln R; Greene LE; Krumova K; Ding Z; Cosa G, Electronic excited state redox properties for BODIPY dyes predicted from Hammett constants: estimating the driving force of photoinduced electron transfer. *J Phys Chem A* 2014, 118 (45), 10622–30. [PubMed: 25066755]
16. Boens N; Leen V; Dehaen W, Fluorescent indicators based on BODIPY. *Chem Soc Rev* 2012, 41 (3), 1130–1172. [PubMed: 21796324]
17. Kowada T; Maeda H; Kikuchi K, BODIPY-based probes for the fluorescence imaging of biomolecules in living cells. *Chem Soc Rev* 2015, 44 (14), 4953–4972. [PubMed: 25801415]
18. Kollmannsberger M; Gareis T; Heintz S; Breu J; Daub J, Electrogenenerated chemiluminescence and proton-dependent switching of fluorescence: Functionalized difluoroboradiazasindacenes. *Angew Chem Int Edit* 1997, 36 (12), 1333–1335.
19. Urano Y; Asanuma D; Hama Y; Koyama Y; Barrett T; Kamiya M; Nagano T; Watanabe T; Hasegawa A; Choyke PL; Kobayashi H, Selective molecular imaging of viable cancer cells with pH-activatable fluorescence probes. *Nat Med* 2008, 15, 104. [PubMed: 19029979]
20. Kollmannsberger M; Rurack K; Resch-Genger U; Rettig W; Daub J, Design of an efficient charge-transfer processing molecular system containing a weak electron donor: spectroscopic and redox

- properties and cation-induced fluorescence enhancement. *Chem Phys Lett* 2000, 329 (5–6), 363–369.
21. Baruah M; Qin W; Vallée RAL; Beljonne D; Rohand T; Dehaen W; Boens N, A Highly Potassium-Selective Ratiometric Fluorescent Indicator Based on BODIPY Azacrown Ether Excitable with Visible Light. *Org Lett* 2005, 7 (20), 4377–4380. [PubMed: 16178537]
 22. Müller BJ; Borisov SM; Klimant I, Red- to NIR-Emitting, BODIPY-Based, K⁺-Selective Fluoroionophores and Sensing Materials. *Adv Funct Mater* 2016, 26 (42), 7697–7707.
 23. Lin Q; Buccella D, Highly selective, red emitting BODIPY-based fluorescent indicators for intracellular Mg²⁺ imaging. *J Mater Chem B* 2018, 6 (44), 7247–7256. [PubMed: 30740225]
 24. Basari N; Baruah M; Qin W; Metten B; Smet M; Dehaen W; Boens N, Synthesis and spectroscopic characterisation of BODIPY® based fluorescent off–on indicators with low affinity for calcium. *Org Biomol Chem* 2005, 3 (15), 2755–2761. [PubMed: 16032354]
 25. Kamiya M; Johnsson K, Localizable and Highly Sensitive Calcium Indicator Based on a BODIPY Fluorophore. *Anal Chem* 2010, 82 (15), 6472–6479. [PubMed: 20590099]
 26. Zeng L; Miller EW; Pralle A; Isacoff EY; Chang CJ, A Selective Turn-On Fluorescent Sensor for Imaging Copper in Living Cells. *J Am Chem Soc* 2006, 128 (1), 10–11. [PubMed: 16390096]
 27. Wu Y; Peng X; Guo B; Fan J; Zhang Z; Wang J; Cui A; Gao Y, Boron dipyrromethene fluorophore based fluorescence sensor for the selective imaging of Zn(ii) in living cells. *Org Biomol Chem* 2005, 3 (8), 1387–1392. [PubMed: 15827633]
 28. Dodani SC; He Q; Chang CJ, A Turn-On Fluorescent Sensor for Detecting Nickel in Living Cells. *J Am Chem Soc* 2009, 131 (50), 18020–18021. [PubMed: 19950946]
 29. Sun Z-N; Liu F-Q; Chen Y; Tam PKH; Yang D, A Highly Specific BODIPY-Based Fluorescent Probe for the Detection of Hypochlorous Acid. *Org Lett* 2008, 10 (11), 2171–2174. [PubMed: 18447382]
 30. Belzile MN; Godin R; Durantini AM; Cosa G, Monitoring Chemical and Biological Electron Transfer Reactions with a Fluorogenic Vitamin K Analogue Probe. *J Am Chem Soc* 2016, 138 (50), 16388–16397. [PubMed: 27998090]
 31. Yang Z; He Y; Lee J-H; Park N; Suh M; Chae WS; Cao J; Peng X; Jung H; Kang C; Kim JS, A Self-Calibrating Bipartite Viscosity Sensor for Mitochondria. *J Am Chem Soc* 2013, 135 (24), 9181–9185. [PubMed: 23713894]
 32. Miller EW; Lin JY; Frady EP; Steinbach PA; Kristan WB Jr.; Tsien RY, Optically monitoring voltage in neurons by photo-induced electron transfer through molecular wires. *Proc Natl Acad Sci U S A* 2012, 109 (6), 2114–9. [PubMed: 22308458]
 33. Woodford CR; Frady EP; Smith RS; Morey B; Canzi G; Palida SF; Araneda RC; Kristan WB; Kubiak CP; Miller EW; Tsien RY, Improved PeT Molecules for Optically Sensing Voltage in Neurons. *J Am Chem Soc* 2015, 137 (5), 1817–1824. [PubMed: 25584688]
 34. Deal PE; Kulkarni RU; Al-Abdullatif SH; Miller EW, Isomerically Pure Tetramethylrhodamine Voltage Reporters. *J Am Chem Soc* 2016, 138 (29), 9085–8. [PubMed: 27428174]
 35. Kulkarni RU; Yin H; Pourmandi N; James F; Adil MM; Schaffer DV; Wang Y; Miller EW, A Rationally Designed, General Strategy for Membrane Orientation of Photoinduced Electron Transfer-Based Voltage-Sensitive Dyes. *ACS Chem Biol* 2017, 12 (2), 407–413. [PubMed: 28004909]
 36. Niu SL; Ulrich G; Ziessel R; Kiss A; Renard PY; Romieu A, Water-soluble BODIPY derivatives. *Org Lett* 2009, 11 (10), 2049–52. [PubMed: 19379006]
 37. Brizet B; Bernhard C; Volkova Y; Rousselin Y; Harvey PD; Goze C; Denat F, Boron functionalization of BODIPY by various alcohols and phenols. *Org Biomol Chem* 2013, 11, 7729. [PubMed: 24113836]
 38. Courtis AM; Santos SA; Guan Y; Hendricks JA; Ghosh B; Szantai-Kis DM; Reis SA; Shah JV; Mazitschek R, Monoalkyl BODIPYs-A Fluorophore Class for Bioimaging. *Bioconj Chem* 2014, 25, 1043–1051.
 39. Li L; Han J; Nguyen B; Burgess K, Syntheses and spectral properties of functionalized, water-soluble BODIPY derivatives. *J Org Chem* 2008, 73 (5), 1963–70. [PubMed: 18271598]
 40. Worries HJ; Koek JH; Lodder G; Lugtenburg J; Fokkens R; Driessen O; Mohn GR, A novel water-soluble fluorescent probe: Synthesis, luminescence and biological properties of the sodium salt of

the 4-sulfonato-3,3',5,5'-tetramethyl-2,2'-pyrromethen-1,1'-BF₂ complex. *Recueil des Travaux Chimiques des Pays-Bas* 1985, 104 (11), 288–291.

41. Komatsu T; Oushiki D; Takeda A; Miyamura M; Ueno T; Terai T; Hanaoka K; Urano Y; Mineno T; Nagano T, Rational design of boron dipyrromethene (BODIPY)-based photobleaching-resistant fluorophores applicable to a protein dynamics study. *Chem Commun* 2011, 47 (36), 10055–7.
42. Wagner RW; Lindsey JS, Boron-dipyrromethene dyes for incorporation in synthetic multi-pigment light-harvesting arrays. *Pure Appl. Chem* 1996, 68 (7), 1373–1380.
43. D'Souza F; Smith PM; Zandler ME; McCarty AL; Itou M; Araki Y; Ito O, Energy Transfer Followed by Electron Transfer in a Supramolecular Triad Composed of Boron Dipyrin, Zinc Porphyrin, and Fullerene: A Model for the Photosynthetic Antenna-Reaction Center Complex. *J Am Chem Soc* 2004, 126 (25), 7898–7907. [PubMed: 15212538]
44. Lou Z; Hou Y; Chen K; Zhao J; Ji S; Zhong F; Dede Y; Dick B, Different Quenching Effect of Intramolecular Rotation on the Singlet and Triplet Excited States of Bodipy. *J. Phys. Chem. C* 2018, 122 (1), 185–193.
45. Bricks JL; Kovalchuk A; Trieflinger C; Nofz M; Büschel M; Tolmachev AI; Daub J; Rurack K, On the Development of Sensor Molecules that Display FeIII-amplified Fluorescence. *J Am Chem Soc* 2005, 127 (39), 13522–13529. [PubMed: 16190715]
46. Romyantsev EV; Alyoshin SN; Marfin YS, Kinetic study of Bodipy resistance to acids and alkalis: Stability ranges in aqueous and non-aqueous solutions. *Inorg Chim Acta* 2013, 408, 181–185.
47. Birkofer L; Bierwirth E; Ritter A, Siliciumorganische Verbindungen .8. Decarbonbenzoxylierungen Mit Triathylsilan. *Chem Ber-Recl* 1961, 94 (3), 821–824.
48. Coleman RS; Shah JA, Chemoselective cleavage of benzyl ethers, esters, and carbamates in the presence of other easily reducible groups. *Synthesis-Stuttgart* 1999, 1399–1400.
49. Dewar MJS, Colour and Constitution .1. Basic Dyes. *J Chem Soc* 1950, (Sep), 2329–2334.
50. Hung J; Liang W; Luo J; Shi Z; Jen AKY; Li X, Rational Design Using Dewar's Rules for Enhancing the First Hyperpolarizability of Nonlinear Optical Chromophores. *J Phys Chem C* 2010, 114 (50), 22284–22288.
51. Olsen S, A quantitative quantum chemical model of the Dewar–Knott color rule for cationic diarylmethanes. *Chem Phys Lett* 2012, 532, 106–109.
52. Boggess SCG, Shivaani S; Siemons Brian A.; , New Molecular Scaffolds for Fluorescent Voltage Indicators. *ACS Chem Biol* 2019, 14, 390–396. [PubMed: 30735344]
53. Bai D; Benniston AC; Clift S; Baisch U; Steyn J; Everitt N; Andras P, Low molecular weight Neutral Boron Dipyrromethene (Bodipy) dyads for fluorescence-based neural imaging. *J Mol Struct* 2014, 1065–1066, 10–15.
54. Sirbu D; Butcher JB; Waddell PG; Andras P; Benniston AC, Locally Excited State–Charge Transfer State Coupled Dyes as Optically Responsive Neuron Firing Probes. *Chem Eur J* 2017, 23 (58), 14639–14649. [PubMed: 28833695]
55. Hansch C; Leo A; Taft RW, A Survey of Hammett Substituent Constants and Resonance and Field Parameters. *Chem Rev* 1991, 91, 165–195.

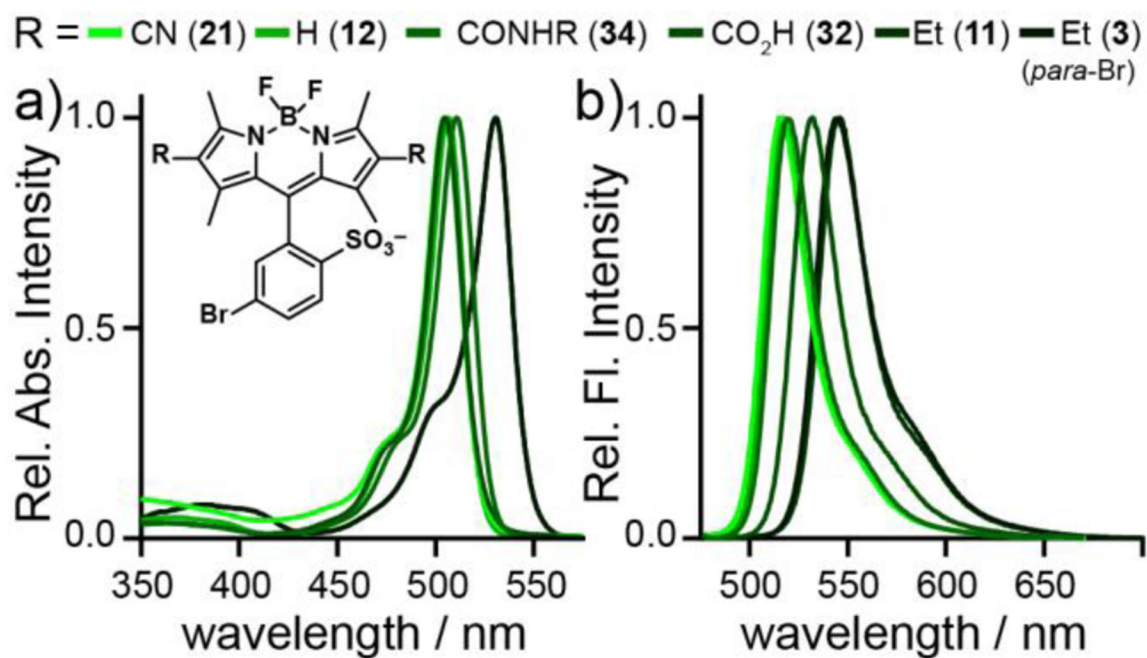


Figure 1. Plots of normalized a) absorption and b) emission of sulfonated BODIPY fluorophores **3**, **11**, **12**, **32**, **34**, and **21**. Spectra were acquired in PBS pH 7.4. Dye concentration is 1 μ M.

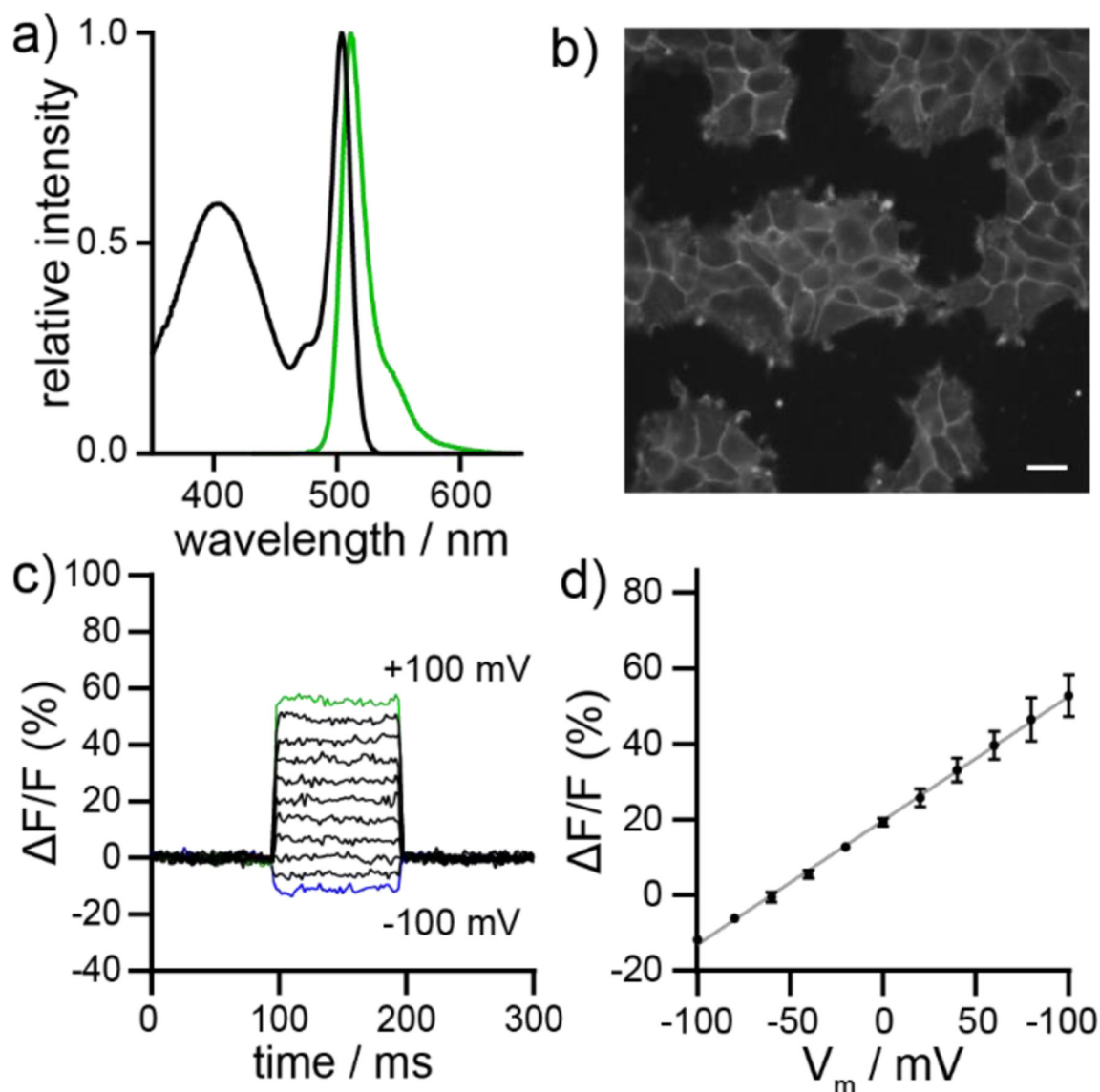


Figure 2.

Spectroscopic, cellular, and functional characterization of BODIPY VF **19**. **a)** Plot of normalized absorbance and emission intensity for BODIPY VF **19** (1 μ M, ethanol). Excitation is provided at 470 nm. **b)** Widefield fluorescence micrograph of HEK cells stained with BODIPY VF **19** (1 μ M). **c)** Plot of fractional change in fluorescence of BODIPY VF **19** ($\Delta F/F$) vs. time for 100 ms hyper- and depolarizing steps (± 100 mV in 20 mV increments) from a holding potential of -60 mV in a single HEK cell under whole-cell voltage-clamp mode. **d)** Plot of fractional change in fluorescence ($\Delta F/F$) vs. final membrane potential. Data represent the mean $\Delta F/F$, \pm S.E.M. for $n = 3$ separate cells. Grey line is the line of best fit.

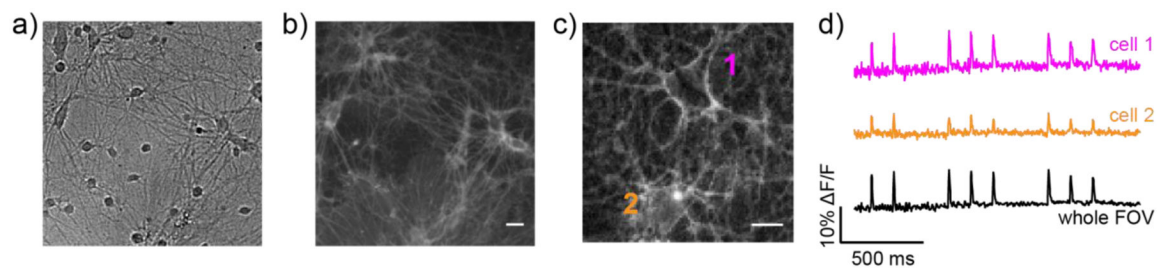


Figure 3.

Voltage imaging in mammalian neurons with BODIPY VF **30**. **a)** Transmitted light and **b)** widefield epifluorescence image of cultured rat hippocampal neurons stained with 500 nM BODIPY VF **30**. Scale bar is 20 μm . **c)** Widefield epifluorescence image of neurons stained with 1 μM BODIPY VF **30** and imaged at 500 Hz. Image is a single frame from this high-speed acquisition. Scale bar is 20 μm . **d)** Plot of fractional change in fluorescence ($\Delta F/F$) for the cells identified in panel (c) or for the entire field of view (FOV).

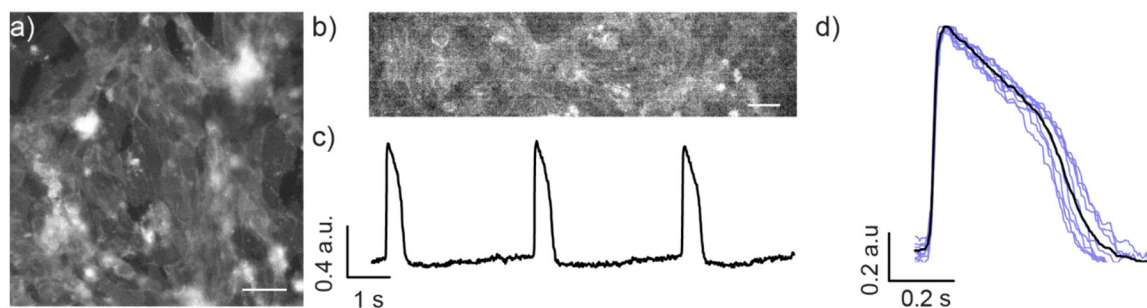
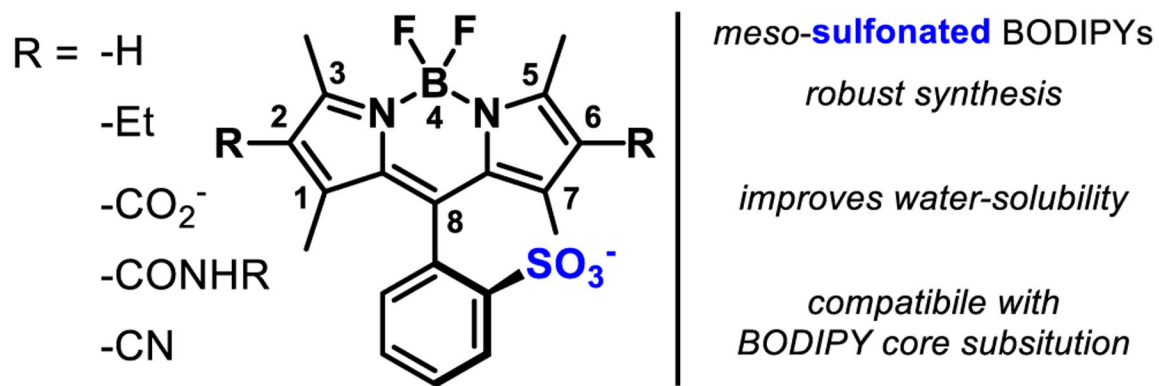
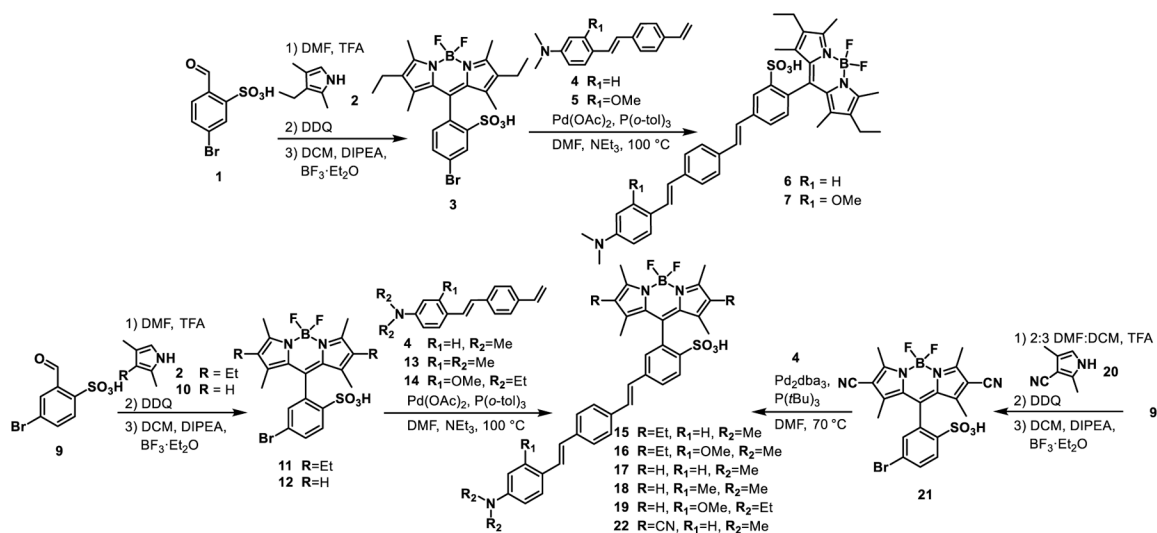


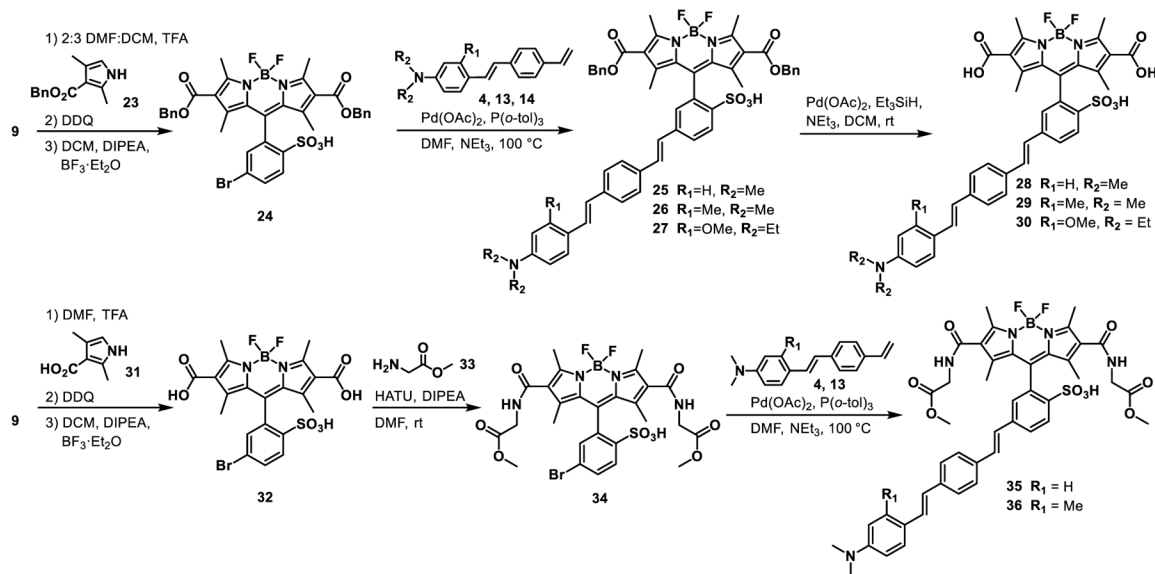
Figure 4. Voltage imaging in human induced pluripotent stem cell-derived cardiomyocytes (hiPSC-CMs) with BODIPY VF **19**. **a)** Widefield, epifluorescence micrograph of hiPSC-CMs stained with 500 nM BODIPY VF **19**. Scale bar is 50 μm . **b)** Single frame of a movie collected at 200 Hz for functional imaging of hiPSC-CM spontaneous action potentials. Scale bar is 50 μm . **c)** Trace of mean pixel intensity (arbitrary fluorescence units, a.u.) from full region of interest (ROI) in panel (b) plotted vs time during 10 second acquisition, corrected for photobleach. **d)** Averaged action potential trace (black) from three 10 second recordings from 3 separate ROIs over individual AP events from each recording (blue).



Scheme 1.
Design of H₂O-soluble BODIPYs



Scheme 2.
Synthesis of BODIPY VoltageFluor dyes with Et, H and CN at the 2,6-positions

**Scheme 3.**

Synthesis of BODIPY VoltageFluor dyes with CO₂H and CONHR at the 2,6-positions.

Table 1.

Spectral properties of sulfonated BODIPYs

	R	λ_{\max} abs	λ_{\max} em	ϵ ($M^{-1} \text{ cm}^{-1}$)	ϕ_f
3	Et	530	544	42000	0.72
11	Et	530	545	44000	0.70
12	H	503	515	57000	0.99
32	CO ₂ H	517	532	56000	0.95
34	CONHCH ₂ CO ₂ Me	507	519	76000	0.92
21	CN	502	517	38000	0.93

All spectral properties acquired in PBS pH 7.4

Properties of BODIPY VoltageFluor (VF) dyes

Table 2.

Name	R	R ₁	isomer	$\lambda_{\max, \text{abs}}^a$	$\lambda_{\max, \text{em}}^a$	ϕ_{fl}^a	% F/F ^{b,c}	Cell brightness ^{c,d}
6	Et	H	<i>para</i>	528	541	0.14	0	0.43 ± 0.02^f
7	Et	OMe	<i>para</i>	527	541	0.07	0	0.76 ± 0.03^f
15	Et	H	<i>meta</i>	528	541	0.15	1.8 ± 0.1	4.4 ± 0.3^f
16	Et	OMe	<i>meta</i>	527	541	0.05	5.4 ± 0.6	0.60 ± 0.03^f
17	H	H	<i>meta</i>	503	518	0.11	2.5 ± 0.1	0.62 ± 0.08
18	H	Me	<i>meta</i>	504	517	0.07	6.2 ± 0.4	1.5 ± 0.2
19	H	OMe	<i>meta</i>	504	512	0.05	33 ± 0.7	1.0 ± 0.1
28	COOH	H	<i>meta</i>	503	516	0.07	4.4 ± 0.2	12 ± 2
29	COOH	Me	<i>meta</i>	503	517	0.03	9.9 ± 0.4	5.1 ± 0.9
30	COOH	OMe	<i>meta</i>	509	522	0.06	24 ± 0.5	7.1 ± 0.8
35	CONHCH ₂ CO ₂ Me	H	<i>meta</i>	508	521	0.06	48 ± 2	1.0 ± 0.1
36	CONHCH ₂ CO ₂ Me	Me	<i>meta</i>	509	521	0.03	5.1 ± 0.4	1.0 ± 0.1
22	CN	H	<i>meta</i>	502	519	0.08	3.8^e	0.34 ± 0.002

^aDetermined in ethanol.^bPer 100 mV depolarization.^cDetermined in HEK cells.^dRelative to **19**, set to a relative brightness of 1.0.^eIncreased exposure time and light intensity required to make measurement.^fPluronic F-127 (0.01%) used during loading.